

Proceedings of the ASME 2022 Conference on Smart Materials,
Adaptive Structures and Intelligent Systems
SMASIS2022
September 12-14, 2022, Dearborn, MI

SMASIS2022-91151

TEMPERATURE COMPENSATION FOR ELECTROMECHANICAL IMPEDANCE SIGNATURES WITH DATA-DRIVEN MODELING

James Femi-Oyetoro 1

Sourabh Sangle²

Pablo Tarazaga²

Mohammad I. Albakri 3*

¹ Department of Mechanical Engineering Tennessee Tech University Cookeville, TN, USA

² Department of Mechanical Engineering Texas A&M University College Station, TX, USA ³ Department of Mechanical Engineering Texas A&M University at Qatar Doha, Qatar

ABSTRACT

Impedance-based structural health monitoring (SHM) is recognized as a non-intrusive, highly sensitive, and modelindependent SHM solution that is readily applicable to complex structures. This SHM method relies on analyzing the electromechanical impedance (EMI) signature of the structure under test over the time span of its operation. Changes in the *EMI signature, compared to a baseline measured at the healthy* state of the structure, often indicate damage. This method has successfully been applied to assess the integrity of numerous civil, aerospace, and mechanical components and structures. However, EMI sensitivity to environmental conditions, the temperature, in particular, has been an ongoing challenge facing the wide adoption of this method. Temperature-induced variation in EMI signatures can be misinterpreted as damage, leading to false positives, or may overshadow the effects of incipient damage in the structure.

In this paper, a new method for temperature compensation of EMI signature is presented. Data-driven dynamic models are first developed by fitting EMI signatures measured at various temperatures using the Vector Fitting algorithm. Once these models are developed, the dependence of model parameters on temperature is established. A parametric data-driven model is then derived with temperature as a parameter. This allows for EMI signatures to be calculated at any desired temperature. The capabilities of this new temperature compensation method are demonstrated on aluminum samples, where EMI signatures are measured at various temperatures. The developed method is found to be capable of temperature compensation of EMI signatures at a broad frequency range.

*Corresponding author. Email: mohammad.albakri@gatar.tamu.edu

Keywords: Structural health monitoring, temperature compensation, electromechanical impedance.

1. INTRODUCTION

Structural health monitoring (SHM) is central for the early detection and identification of damage and degradation of structures. mechanical. aerospace, and civil implementation of SHM systems enhances safety and reliability by enabling condition-based maintenance instead of schedulebased practices. Among the different methods and techniques that have been developed for this purpose over the last few decades, Impedance-based SHM is recognized as a nonintrusive, highly sensitive solution that is readily applicable to complex structures [1,2]. Impedance-based SHM has successfully been applied to detect damage in numerous civil, aerospace, and mechanical components and structures, both in the lab and under real operating conditions. This included composite structures, reinforced concrete, bridges, wind turbine blades, space structures, and railroad track components [3-5]. Electromechanical impedance (EMI) measurements have also been used for nondestructive evaluation of manufactured parts [6], for in situ monitoring of additively manufactured components [7], and as a solution for creating a unique identity of manufactured parts and components in distributed supply chains [8].

Despite the successful implementation of impedance-based SHM, variations in operating and environmental conditions experienced by the structure under test remain a major challenge. In particular, temperature variations have been found to have a drastic impact on the measured EMI signature. Temperature-induced variation in EMI signatures can be

misinterpreted as damage, leading to false positives, or may overshadow the effects of incipient damage in the structure.

To address this challenge, several researchers have investigated and devised temperature compensation techniques. Park et al., proposed a modified root mean square deviation (RMSD) to compensate for the temperature variation that brings about a vertical and horizontal shift of electrical impedance [9]. Baptista et al. studied the frequency and amplitude changes in EMI signatures of aluminum specimens at temperatures ranging from 25°C to 102°C [10]. They found that temperature changes lead to a vertical shift in the EMI signatures in addition to changes in the frequency of the resonance peaks. Tekalmaz et al. applied the effective frequency shift technique as a temperature compensation solution for AISI-1080 steel EMI signatures measured at low temperatures, ranging from -45°C and -10°C [11]. Similar results were reported by Huynh and Kim, where effective frequency shift to mitigate the effect of temperature the EMI signature of a tendon anchorage measured at different pre-stress levels [12].

In this paper, a new method for temperature compensation of EMI signature utilizing data-driven modeling is presented. Data-driven dynamic models are first developed by fitting EMI signatures measured at various temperatures using the Vector Fitting algorithm. Once these models are developed, the dependence of model parameters on temperature is established. This allows for a temperature-dependent parametric data-driven model to be developed for the structure under test. With this model, the EMI can be calculated at any desired temperature to generate the temperature-compensated EMI signature.

The paper briefly discusses the fundamentals of impedance-based SHM in Sections 2. Section 3 discusses the experimental aspect of this work. The proposed data-driven modeling temperature compensation technique is then discussed in Section 4, where its capabilities are demonstrated. Concluding remarks and future research directions are finally presented in Section 5.

2. ELECTROMECHANICAL IMPEDANCE

Impedance-based SHM is an active, vibration-based, damage-identification technique. As an active technique, impedance-based SHM excites the structure under test at the desired frequency range using piezoelectric transducers. Due to the coupled electromechanical characteristics of piezoelectric materials, changes in the dynamic response of the structure under test are reflected on the easily measured electrical impedance of the piezoelectric transducer attached to the structure. The fundamental basis of impedance-based SHM is that the presence of damage will alter the mass, stiffness, and damping characteristics of the structure under test, which in turn alters its dynamic response as well as the measured EMI signature. Thus, changes in the host structure can be detected. Figure shows a schematic of a piezoelectric transducer attached to the joint bar of an insulated rail joint. At the frequency range

of interest, the structure under test can be approximated as a single-degree-of-freedom system, as shown in the figure, with modal mass, stiffness, and damping denoted by m_r , k_r , and ζ_r , respectively. Assuming linear piezoelectricity, the constitutive equations of the piezoelectric materials operating in 1-3 mode can be expressed as [13]

$$\begin{array}{c} \varepsilon_{11}=s_{11}^E\sigma_{11}+d_{13}E_3\\ D_3=(d^T)_{31}\sigma_{11}+\epsilon_{33}^\sigma E_3\ ,\\ \end{array} \tag{1}$$
 where ε_{11} is the strain tensor component in the 1-direction, σ_{11}

where ε_{11} is the strain tensor component in the 1-direction, σ_{11} is the corresponding component of the work-conjugate stress tensor, D_3 is the electric displacement in the 3-direction, E_3 is the electric field in the 3-direction, d_{13} is the piezoelectric coupling coefficient, s_{11}^E is the complex mechanical compliance of the material measured at zero electric field. $\varepsilon_{33}^{\sigma}$ is the complex permittivity measured at zero stress.

The electrical impedance of the piezoelectric transducer, $Z(\omega)$, is directly related to the mechanical impedance of the structure to which the transducer is attached, Z_{st} . Following Liang and Rogers [2], this dependence can be expressed as follows:

$$Z(\omega) =$$

$$\left[i\omega \frac{bl}{h} \left(\frac{d_{13}^2}{s_{11}^E} \left(\frac{tan(kl)}{kl} \left(\frac{Z_{pzt}}{Z_{pzt} + Z_{st}}\right) - 1\right) + \bar{\epsilon}_{33}^{\sigma}\right)\right]^{-1} \tag{2}$$

where $Z_{pzt} = -iblh(s_{11}^E \omega \ tan(kl)/kl)^{-1}$ is the short circuit impedance of the piezoelectric transducer, $k = \omega \sqrt{\rho \bar{s}_{11}^E}$ is the wavenumber corresponding to the first symmetric mode with ω

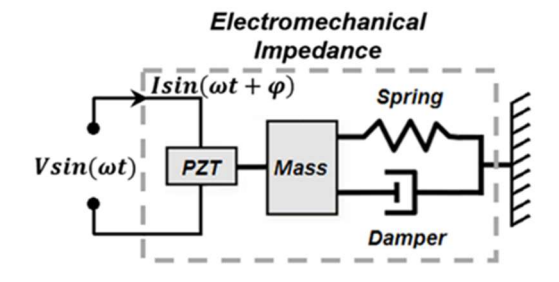


Figure 1. A single-degree-of-freedom representation of electromechanical impedance measurements.

being the angular frequency and ρ being the density of the piezoelectric material. $Z_{st}=2\zeta_r(k_rm_r)^{1/2}+i(m_r\omega^2-k_r)/\omega$ is the mechanical impedance of the single-degree-of-freedom approximate model of the structure under test. b,h and 2l are the piezoelectric patch width, thickness, and length, respectively.

As suggested by equation 2, the EMI signature depends on the material properties of the piezoelectric transducer, its capacitance/permittivity in particular. Such properties are known to be impacted by temperature variations, thus such variations will lead to changes, mostly vertical shifts, in the EMI signature. Furthermore, temperature variations are also known to affect the mechanical properties of the piezoelectric transducer and the structure under test, as well as the bonding layer between them, which further impacts the measured EMI signature.

3. EXPERIMENTAL SETUP

To investigate the effects of temperature on EMI measurements, a simple experiment was conducted on an aluminum beam with the dimensions 76.2mm × 12.7mm × 6.35mm. An epoxy adhesive was used to bond the monolithic piezoelectric patch of dimensions 12.6mm × 12.6mm to one end of the specimen, as shown in Figure 2. The piezoelectric transducer was affixed to the structure with a gap of 1mm from the end of the structure. A Ney Centurion Qex laboratory furnace is used to provide a controlled heating enclosure for EMI measurement at the different temperatures considered in the study. The EMI signatures of the specimens are measured using a Zurich Instruments MFIA impedance analyzer connected to the LabOne computer interface. Figure 3 shows the schematic of the experimental setup used in this study.



Figure 2. Instrumented Aluminum specimen.

The EMI signatures are measured over the frequency range of 1kHz to 100kHz with a 20Hz resolution. Experiments are conducted to assess the influence of temperature on EMI signatures and afterward to propose a temperature compensation method. It is worthy to highlight that measurements are acquired after a duration of 20 minutes, at least, after the laboratory furnace has attained the set temperature. This is to allow for all specimens inside the furnace chamber to reach steady-state temperature. EMI signatures are measured at 5 different temperatures ranging from 25°C to 45°C with 5°C increments.

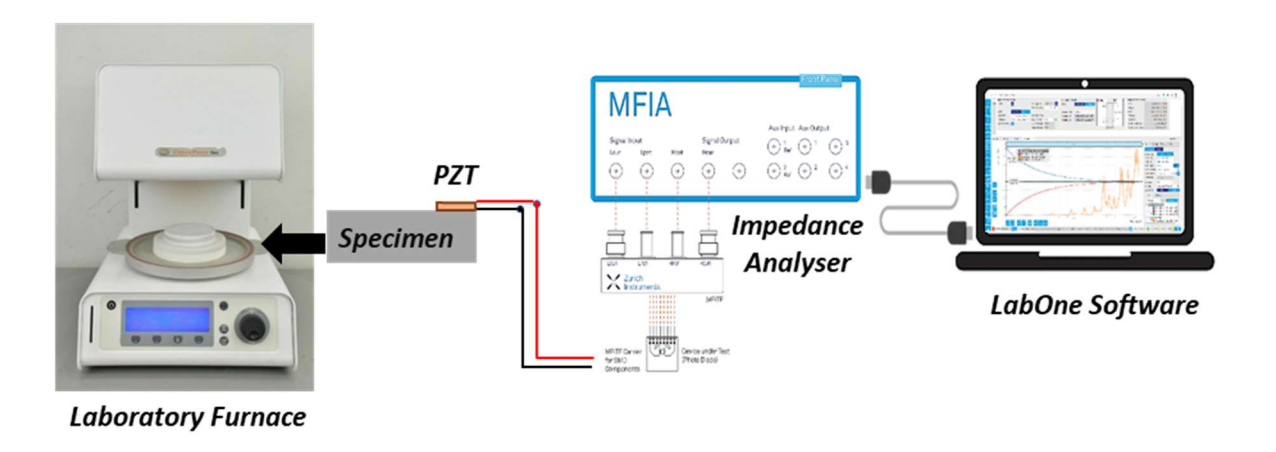


Figure 3. Electromechanical impedance measurement setup with controlled temperature.

For all temperatures considered in this study, the EMI signatures are measured three times to verify the repeatability of measurement. The set temperature was adjusted on the laboratory furnace from the control panel; however, the temperature was monitored using a thermocouple probe with a multimeter to eliminate any form of calibration error. Both the laboratory furnace and thermocouple multimeter showed excellent consistency in terms of temperature measurement within the furnace chamber.

4. RESULT AND DISCUSSION

4.1. Temperature Effects on EMI Signatures

The real part of the EMI signature of the specimen measured at different temperatures from 25°C to 45°C is shown in Figure 4. It is observed that there exists a vertical shift in the impedance signature along with a horizontal frequency shift. The frequency shift is predominantly observed at the resonance peaks. The measured EMI signatures also show a decrease in the magnitude of the real part of the impedance as the temperature increases. These trends are found to be consistent across the entire frequency range considered in the study. The

close-up plots in Figure 4 clearly show these trends. The EMI signatures measured at a given temperature showed excellent repeatability, confirming the consistency and accuracy of the approach followed when changing environmental conditions.

4.2. Data-driven Rational Approximation for Temperature Compensation

Let $Z(j\omega) \in \mathbb{C}$ denote the complex EMI signature of a dynamical system sampled at the frequencies $\omega_1, \omega_2, ..., \omega_N$ which is measured at a given temperature T_n . Given these samples, a rational function, $\tilde{Z}(s) = \frac{n(s)}{d(s)}$, of degree-r is constructed such that least-squares error is minimized

$$\min \sum_{l=1}^{N} \left| Z(j\omega_l) - \tilde{Z}(j\omega_l) \right|^2$$
 (3)

To achieve this, the Vector Fitting method of Gustavsen et al. is used [14, 15]. Since the unknowns appear both in n(s) and d(s), the minimization problem is a nonlinear least-squares problem that is solved iteratively by solving a sequence of linear problems until convergence is achieved. The Vector Fitting method used in this study uses the barycentric form for a rational function. Upon convergence, the final rational approximation is given by

$$\tilde{Z}(s) = \sum_{m=1}^{r} \frac{\phi_m}{s - \lambda_m} = C(sI - A)^{-1}B$$

$$, \quad \phi_m, \ \lambda_m \in \mathbb{C}$$
(4)

In this work, a set of data-driven models are obtained for the part under test, one corresponding to each measurement temperature. The dependence of the models' poles and residues, λ_m and ϕ_m , on temperature is then established. Once this is done, i.e. the functions $\lambda_m(T)$ and $\phi_m(T)$ are obtained, the EMI signature at any temperature of interest can be calculated. When this is done for the healthy signature of the structure, known as the baseline signature, a temperature-compensated (corrected) baseline can be obtained. Temperature-corrected baseline is then used to guide damage detection and identification efforts.

Using the Vector Fitting algorithm, data-driven models were developed to fit the EMI signatures measured at three of the five temperatures considered in the study, these are 25°C, 35°C, and 45°C. These models are then used to establish the dependence of poles and residues on temperature. The remaining two EMI signatures, measured at 30°C and 40°C, are used for validation. This analysis is applied to the EMI signature measured over the frequency range of 58 kHz to 62 kHz, focusing on a single impedance peak. The analysis can be extended to the entire frequency range at the cost of increasing model order. Figure 5 shows the EMI signature, measured at 45°C, along with the fit obtained with the Vector Fitting method for the frequency range specified earlier. The data-driven model output is in good agreement with the measured data. Similar models are obtained using the measurements conducted at 25°C and 35°C.

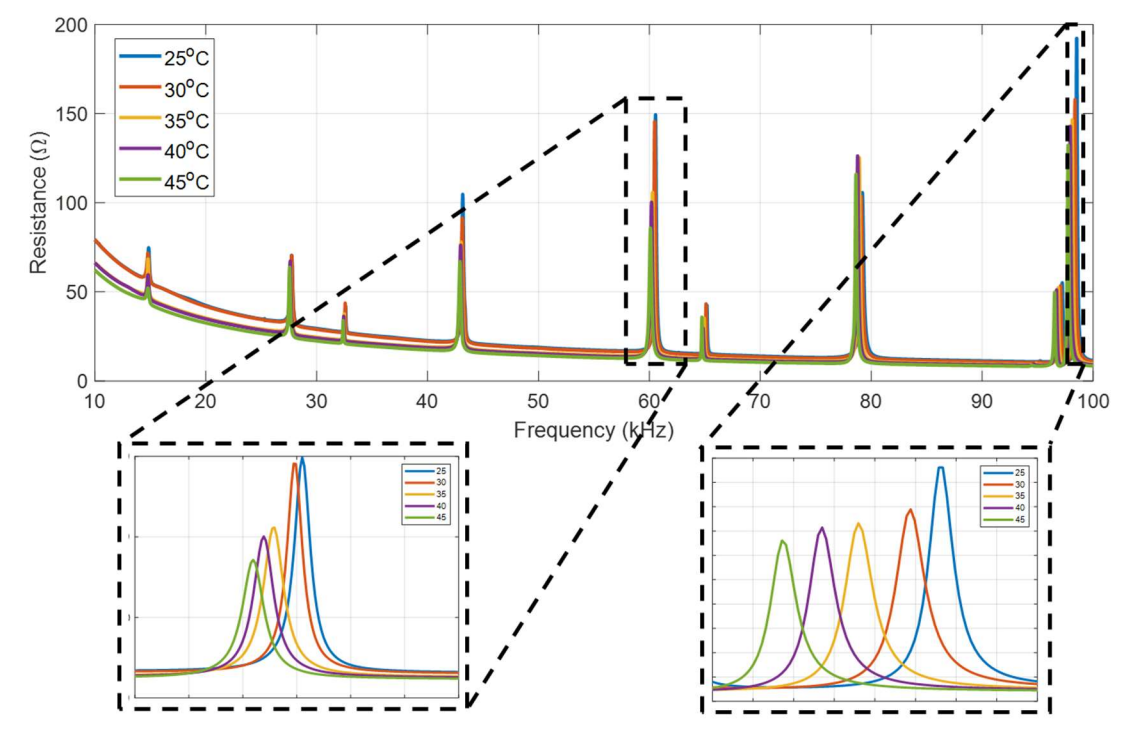


Figure 4. Variation in EMI signatures with temperature.

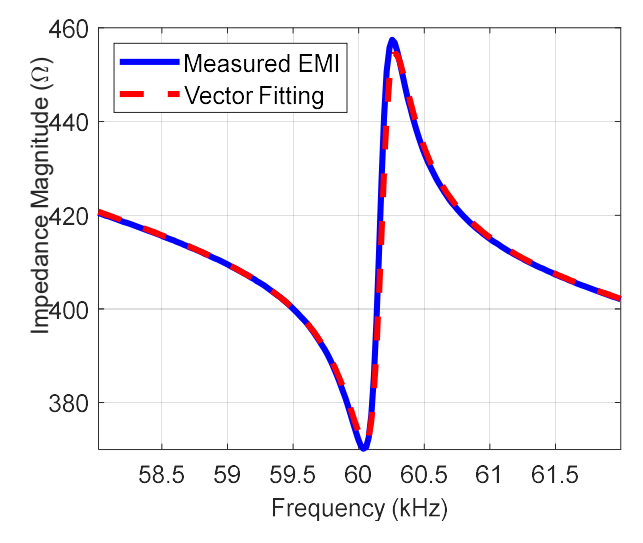
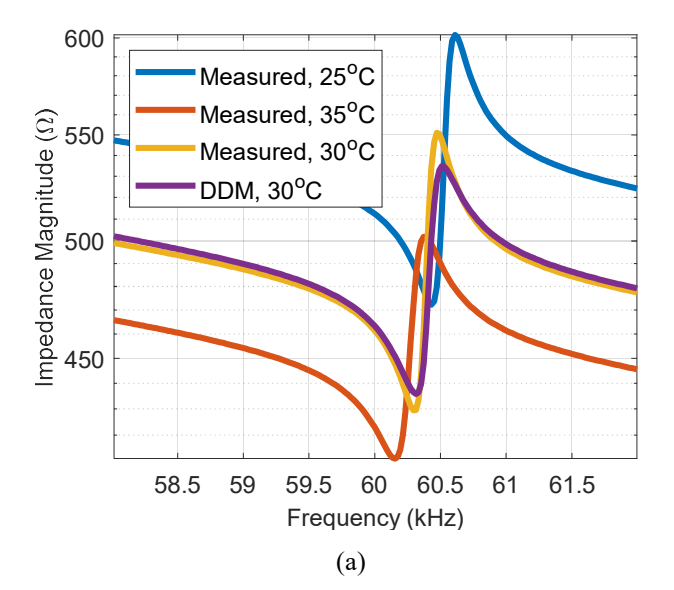


Figure 5. Experimentally measured EMI signature at 45°C along with the Vector Fitting results.

Once data-driven models are developed for the temperatures 25°C, 35°C, and 45°C EMI signatures, model poles and residues are stored. The poles and residues are complex-valued in form of complex conjugate pairs. These are then used to calculate the poles and residues at intermediate temperatures using linear interpolation. This is done for both the real and imaginary components of the poles/residues. To demonstrate the capabilities of this approach, the 25°C and 35°C EMI signatures are used to predict the EMI signature at 30°C. The results are shown in Figure 6.a. The predicted EMI signature, labeled as DDM in the figure, is compared to the measured response at that temperature, and both are found to be in good agreement. A similar exercise is done using the 35°C and 45°C EMI signatures are to predict the EMI signature at 40°C, the results are shown in Figure 6.b.

The results show that the developed temperature compensation technique is capable of compensating for the temperature effects on EMI signatures accurately, using a very limited number of measurements. The temperature-compensated signature can be used as the baseline to which new measurements taken at a given temperature are compared for damage detection or part identification purposes.

Although the pole/residue-temperature relationship is not perfectly described by a first-order polynomial, the results of the linear interpolation are found to be satisfactory. Higher-order interpolation functions will be investigated in future studies to improve the accuracy of the temperature compensated EMI signatures.



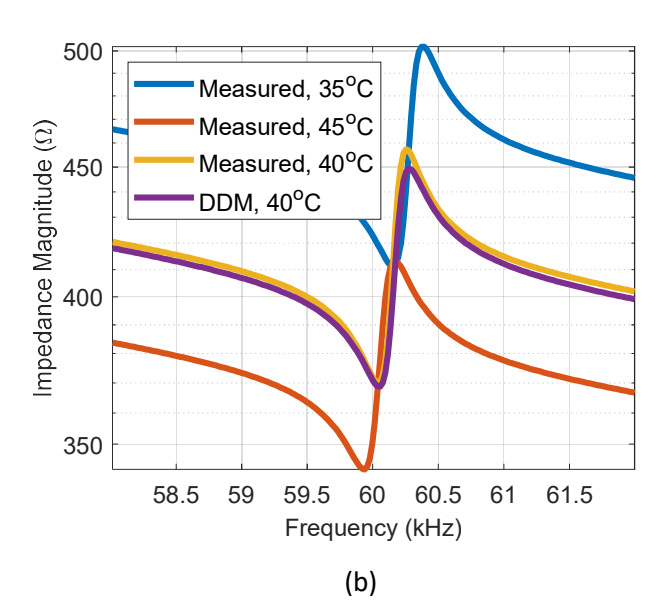


Figure 6. DDM temperature compensation at (a) 30°C and (b) 40°C

5. CONCLUSIONS

This paper presents a new temperature compensation method for EMI signatures. This method utilizes data-driven modeling, namely the Vector Fitting method, to generate models capable of describing the EMI signatures measured at various temperatures. Once these models are developed, the dependence of model poles and residues on temperature is established. This allows for a temperature-dependent parametric data-driven model to be developed for the structure under test. Linear interpolation is conducted to predict the poles and residues at any temperature in the range defined by the measured data.

The developed temperature compensation technique is found to be capable of compensating for the temperature effects on EMI signatures accurately, using a very limited number of measurements. The temperature-compensated signature can be used as the baseline to which new measurements taken at a given temperature are compared for damage detection or part identification purposes.

Future studies will investigate higher-order interpolation functions to improve the accuracy of the temperature compensated EMI signatures. The technique will also be used with various materials and geometries to better identify its capabilities and limitations.

REFERENCES

- [1] G. Park, H. Sohn, C. R. Farrar, and D. J. Inman, 2003, "Overview of piezoelectric impedance-based health monitoring and path forward," Shock Vib. Dig., vol. 35, no. 6, pp. 451–464.
- [2] C. Liang, F. P. Sun, and C. A. Rogers, 1994, "An Impedance Method for Dynamic Analysis of Active Material Systems," J. Vib. Acoust., vol. 116, no. 1, pp. 120–128.
- [3] B. Han, Y. Wang, S. Dong, L. Zhang, S. Ding, X. Yu, and J. Ou, 2015, "Smart concretes and structures: A review," J. Intell. Mater. Syst. Struct., vol. 26, no. 11, pp. 1303–1345.
- [4] S. G. Taylor, K. Farinholt, M. Choi, H. Jeong, J. Jang, G. Park, J.-R. Lee, and M. D. Todd, 2014, "Incipient crack detection in a composite wind turbine rotor blade," J. Intell. Mater. Syst. Struct., vol. 25, no. 5, pp. 613–620.
- [5] M.I. Albakri, V. Malladi, A. Woolard, and P. A. Tarazaga "In-field implementation of impedance-based structural health monitoring for insulated rail joints", Proc. SPIE 10169, Nondestructive Characterization and Monitoring of Advanced Materials, Aerospace, and Civil Infrastructure 2017, 101690E
- [6] Albakri, M.I., Sturm, L.D., Williams, C.B. and Tarazaga, P.A., 2017. Impedance-based non-destructive evaluation of additively manufactured parts. Rapid Prototyping Journal, I, vol. 23, pp. 589-601.
- [7] Sturm, L.D., Albakri, M.I., Tarazaga, P.A. and Williams, C.B., 2019. In situ monitoring of material jetting additive manufacturing process via impedance based measurements. Additive Manufacturing, 28, pp.456-463.
- [8] Sandborn, M., Olea, C., White, J., Williams, C., Tarazaga, P.A., Sturm, L., Albakri, M. and Tenney, C., 2021. Towards secure cyber-physical information association for parts. Journal of Manufacturing Systems, 59, pp.27-41.
- [9] G. Park, K. Kabeya, H. H. Cudney, and D. J. Inman, "Impedance-based structural health monitoring for temperature varying applications," JSME Int. Journal, Ser. A Mech. Mater. Eng., 1999, doi: 10.1299/jsmea.42.249.
- [10] F. G. Baptista, D. E. Budoya, V. A. D. de Almeida, and J. A. C. Ulson, "An experimental study on the effect of temperature on piezoelectric sensors for impedance-based

- structural health monitoring," Sensors (Switzerland), 2014, doi: 10.3390/s140101208.
- [11] M. Tekkalmaz, G. Haydarlar, and M. A. Sofuoğlu, "A statistical analysis of temperature compensation for piezoelectric sensor bonded to AISI-1080 material," Proc. Inst. Mech. Eng. Part C J. Mech. Eng. Sci., 2021, doi: 10.1177/0954406220978250.
- [12] T. C. Huynh, K. S. Lee, and J. T. Kim, "Local dynamic characteristics of PZT impedance interface on tendon anchorage under prestress force variation," 2015, doi: 10.12989/sss.2015.15.2.375.
- [13] D. J. Leo, Engineering analysis of smart material systems. Hoboken, N.J. Wiley, 2007.
- [14] Gustavsen, B., and Semlyen, A., 1999. "Rational approximation of frequency domain responses by vector fitting". IEEE Transactions on power delivery, 14(3), pp. 1052–1061
- [15] Gustavsen, B., 2006. "Improving the pole relocating properties of vector fitting". IEEE Transactions on Power Delivery, 21(3), pp. 1587–1592.